The association between BOLD-based cerebrovascular reactivity (CVR) and end-tidal CO_2 in healthy subjects

Xirui Hou [a,b], Peiying Liu [b,c], Yang Li [b], Dengrong Jiang [a,b], Jill B. De Vis [b], Zixuan Lin [a,b], Sandeepa Sur [b], Zachary Baker [a,b], Deng Mao [c,d], Harshan Ravi [e], Karen Rodrigue [f], Marilyn Albert [g], Denise C. Park [f], Hanzhang Lu [a,b,c,*]

[a] Department of Biomedical Engineering, Johns Hopkins University School of Medicine, Baltimore, MD, USA
[b] The Russell H. Morgan Department of Radiology, Johns Hopkins University School of Medicine, Baltimore, MD, USA
[c] F.M. Kirby Research Center for Functional Brain Imaging, Kennedy Krieger Institute, Baltimore, MD, USA
[d] Philips Healthcare, Baltimore, MD, USA
[e] Department of Cancer Physiology, Moffitt Cancer Research Center, Tampa, FL, USA
[f] Center for Vital Longevity, School of Behavioral and Brain Sciences, University of Texas at Dallas, Dallas, TX, USA
[g] Department of Neurology, Johns Hopkins University School of Medicine, Baltimore, MD, USA

ARTICLE INFO

ABSTRACT

Cerebrovascular reactivity (CVR) mapping using CO_2-inhalation can provide important insight into vascular health. At present, blood-oxygenation-level-dependent (BOLD) MRI acquisition is the most commonly used CVR method due to its high sensitivity, high spatial resolution, and relatively straightforward processing. However, large variations in CVR across subjects and across different sessions of the same subject are often observed, which can cloud the ability of this promising measure in detecting diseases or monitoring treatment responses. The present work aims to identify the physiological components underlying the observed variability in CVR data. When studying the association between CVR value and the subject's CO_2 levels in a total of $N = 253$ healthy participants, we found that CVR was lower in individuals with a higher basal end-tidal CO_2, $EtCO_2$ (slope $= -0.0036 \pm 0.0008\%/mmHg^2$, $p < 0.001$), or with a greater $EtCO_2$ change ($\Delta EtCO_2$) with hypercapnic condition (slope $= -0.0072 \pm 0.0018\%/mmHg^2$, $p < 0.001$). In a within-subject setting, when studying the CVR difference between two repeated scans (with repositioning) in relation to the corresponding differences in basal $EtCO_2$ and $\Delta EtCO_2$ ($n = 11$), it was found that CVR values were lower if the basal $EtCO_2$ or $\Delta EtCO_2$ during that particular scan session was greater. The present work suggests that basal physiological state and the level of hypercapnic stimulus intensity should be considered in application studies of CVR in order to reduce inter-subject and intra-subject variations in the data. Potential approaches to use these findings to reduce noise and augment sensitivity are proposed.

1. Introduction

With a growing need for biomarkers in large-vessel and small-vessel brain diseases, there has been a surging interest in mapping cerebrovascular reactivity (CVR) in recent years. CVR refers to the ability of cerebral vessels to dilate or constrict in response to vasoactive challenges such as hypercapnia or injection of acetazolamide. It is a marker of vascular reserve and is complementary to basal measures of brain hemodynamics such as cerebral blood flow (CBF), cerebral blood volume

(CBV) and oxygen extraction fraction (OEF) (Chen, 2018; Liu et al., 2019). Non-invasive measurements of CVR have found clinical applications in a broad spectrum of brain diseases including arterial stenosis (De Vis et al., 2015; Liu et al., 2017; Mandell et al., 2008), stroke (Geranmayeh et al., 2015; Taneja et al., 2019), brain tumors (Fierstra et al., 2016), traumatic brain injury (Chan et al., 2015), dementia (Yezhuvath et al., 2012), multiple sclerosis (Marshall et al., 2014), and normal aging (Lu et al., 2011; McKetton et al., 2018; Peng et al., 2018). Additionally, CVR has also been used for the calibration of fMRI signal and estimation

---

of cerebral metabolic rate of oxygen consumption ($CMRO_2$) (Bright et al., 2017; Davis et al., 1998; Gauthier and Hoge, 2013; Hoge et al., 1999; Liu et al., 2013; Murphy et al., 2011).

The most commonly used approach to measure CVR is to employ hypercapnic challenge inside the MRI scanner while continuously collecting end-tidal CO_2 ($EtCO_2$) and Blood-Oxygenation-Level-Dependent (BOLD) images (Bright et al., 2011; Fierstra et al., 2013; Liu et al., 2019; Yezhuvath et al., 2009). A regression analysis between $EtCO_2$ and BOLD signal time-courses will then yield a CVR index in the units of %/mmHg CO_2. While the data collection and analysis methods of CVR MRI are straightforward due to the robustness of both the $EtCO_2$ and BOLD signals, there have been observations of substantial variations in CVR values across normal subjects (Bright et al., 2011; Halani et al., 2015; Lu et al., 2011; Murphy et al., 2011), sometimes even across different sessions of the same subjects (Bright and Murphy, 2013; Peng et al., 2018). To date, the physiological mechanisms of these variations have not been elucidated.

A better understanding of normal variations in CVR is of importance in both clinical and basic science applications of this promising technique. First, variations in CVR data increase "noise level" when comparing normal to abnormal populations and reduce the statistical power to detect pathology-related differences. They may also preclude personalized determination of abnormalities. Second, a better understanding of CVR variations will allow more informed interpretation of CVR results. One can ascertain whether the observed CVR change is truly due to vascular reserve alterations or due to differences in its physiological modulators. Finally, identification of physiological modulators of CVR will help improve the reliability of fMRI calibration and normalization, as fMRI and its calibration scans are typically performed under different experimental settings (e.g. with and without mask, mouthpiece, etc.).

Given that the BOLD MRI signal is a complex function of CBF (Bhogal et al., 2014; Sobczyk et al., 2014) and that CBF itself may be a non-linear function of $EtCO_2$ (Tancredi and Hoge, 2013), we hypothesize that BOLD-based CVR measure is dependent on both basal $EtCO_2$ ($bEtCO_2$) and its change due to hypercapnia ($\Delta EtCO_2$) in healthy subjects. The goal of the present study is, therefore, to investigate the effects of $bEtCO_2$ and $\Delta EtCO_2$ on CVR, in both between-subjects and within-subject settings. To study the between-subject effect, we examined the association between CVR and the above-mentioned physiological factors using data from 4 CVR studies that we had performed, with an aggregated sample size of 253 healthy subjects. To study the within-subject effect, we examined CVR values from repeated CVR scans and investigate if their differences are dependent on differences in $bEtCO_2$ and $\Delta EtCO_2$. Finally, numerical simulations were also performed using a BOLD biophysical model to verify the experimental findings.

2. Materials and methods

The present work consists of two major components. One is to study the inter-subject relationship between CVR and $EtCO_2$; the other is on their intra-subject relationship.

2.1. Inter-subject variations in CVR and their dependence on end-tidal CO_2

2.1.1. Experiment

The datasets used for this study consist of data from 4 independent studies totaling 253 adults ranging from 20 to 88 years old (Table 1). All study procedures were approved by the Institutional Review Board of the Johns Hopkins University or The University of Texas at Dallas. The participants gave informed written consent before being enrolled.

All CVR experiments were conducted on Philips 3T MRI (Achieva). Studies 1, 2, and 3 were performed on a scanner at Johns Hopkins University, while Study 4 was performed on a scanner at University of Texas. Gas delivery during the experiments used an identical apparatus and was based on an inspired 5% CO_2 challenge as described in previous studies

Table 1
Summary of demographic and imaging parameters of the four studies performed in this work.

	Study 1	Study 2	Study 3	Study 4
N	11	10	25	207
Age, yo (SD)	24.1 (3.2)	28 (6.8)	68.8 (6.0)	50.9 (19.9)
Gender				
Male	7	3	8	82
Female	4	7	17	125
$EtCO_2$				
Basal $EtCO_2$, mmHg (SD)	37.9 (4.0)	36.6 (4.2)	36.0 (3.8)	38.5 (4.3)
$\Delta EtCO_2$, mmHg (SD)	9.3 (1.8)	8.1 (1.1)	9.3 (1.8)	9.1 (2.0)
Image parameter				
Repetition Time, ms	1500	1500	1500	2000
Echo Time, ms	21	21	21	25
Flip Angle	90°	90°	90°	80°
Field of View, mm^2	205 × 205	205 × 205	220 × 220	220 × 220
Slice Number	36	36	36	43
Slice-thickness, mm	3.5	3.5	3.8	3.5
Gap, mm	0	0	0	0
In-plane resolution, mm^2	3.2 × 3.2	3.2 × 3.2	3.4 × 3.4	3.4 × 3.4
Scan Duration, min	7	5	7	7

(Lu et al., 2014). Briefly, subjects were fitted with a nose clip, and breathed approximately 1 min of 5% CO_2 gas mixture (21% O_2, 74% N_2) and 1 min of room-air in an interleaved fashion through a mouthpiece (Fig. 1a). The CO_2 gas mixture was contained in Douglas bags and delivered through a two-way non-rebreathing valve (Hans Rudolph, 2600 series, Shawnee, KS). A research assistant was inside the magnet room throughout the experiment to switch the valve and monitor the subjects. The $EtCO_2$ was recorded throughout the experiment using a capnograph device, an example of which is shown in Fig. 1b.

In addition to the BOLD CVR scan, each subject in each study also received a T1-weighted scan for anatomic reference. The T1-weighted scan used the following imaging parameters which were identical in all four studies: magnetization-prepared rapid gradient-echo sequence (MPRAGE), TR = 8.1 ms, TE = 3.7 ms, shot interval = 2100 ms, FA = 12°, FOV = 204 × 256 mm^2, 160 slices with 1 × 1 × 1 mm^3 voxels.

Table 1 summarizes participant demographic information and imaging parameters of the four studies, which were performed under different projects. None of these projects have published data related to the CO_2 effect that is of interest in this work. Study 2 used two CO_2 inhalation blocks with a scan duration of 5 min, while the other studies used three CO_2 blocks with a 7-min scan duration. We also want to note that the TEs used for these CVR studies were slightly shorter than typical fMRI experiments. This was to reduce the signal contrast between parenchymal and cerebrospinal fluid (CSF) spins and minimize the sensitivity of the sequence to changes in cerebral blood volume (CBV) (Ravi et al., 2016; Thomas et al., 2013).

2.1.2. Data processing

Image analysis was conducted using the software Statistical Parametric Mapping (SPM, University College London, UK) and in-house MATLAB (MathWorks, Natick, MA) scripts. The BOLD CVR data first underwent standard pre-processing steps including slice timing correction, realignment, skull stripping, normalization to Montreal Neurologic Institute (MNI) standard brain space via MPRAGE image, and spatial smoothing using a Gaussian filter with a full-width half-maximum of 4 mm (Hou et al., 2019).

The data were further processed to compute CVR maps (Liu et al., 2019). Briefly, the $EtCO_2$ time course was temporally aligned with the global BOLD time series to account for the time it takes for CO_2 to travel from the lung (where the $EtCO_2$ was recorded) to the brain (where the BOLD signal was recorded). Next, a multi-linear regression was performed using

$$BOLD(t) = \beta_0 + \beta_1 \cdot EtCO_{2,aligned}(t) + \beta_2 \cdot t \qquad (1)$$
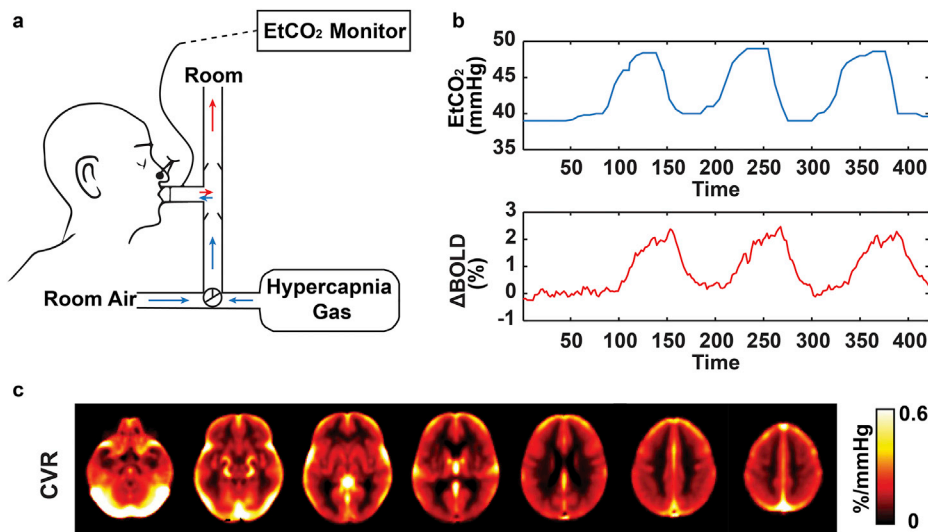
Fig. 1. Illustration of Cerebrovascular Reactivity (CVR) measurement and data. (a) Schematic illustration of gas delivery and recording inside the MRI. (b) Representation data of $EtCO_2$ and whole-brain BOLD signal time course. (c) CVR map averaged over the entire cohort (N = 253).

where BOLD(t) is the BOLD MRI signal time course, t is time, and β_0, β_1, β_2 are coefficients to be estimated. Note that the term $\beta_2 \cdot t$ was added to account for potential drifting of the signal.

CVR can then be computed as

$$CVR = \frac{\beta_1}{\beta_0 + bEtCO_2 \cdot \beta_1} \quad (2)$$

We note that CVR was not calculated as $\frac{\beta_1}{\beta_0}$, but instead contains the $bEtCO_2 \cdot \beta_1$ term, so that the measured CVR is in reference to basal $EtCO_2$ state under room air, rather than in reference to a non-physiological state of $EtCO_2$ of 0 mmHg. However, it should be pointed out that, for practical purposes, the $bEtCO_2 \cdot \beta_1$ term is much smaller than β_0 (-0.7 ± 0.2% in our data). Thus, researchers can also use $\frac{\beta_1}{\beta_0}$ to compute CVR value with minimal differences. Considering the typical $EtCO_2$ time course in our study (e.g. Fig. 1b) and certain fluctuations, we defined $bEtCO_2$ as the average of the lowest 25% of the $EtCO_2$ time course. Similarly, the $EtCO_2$ during hypercapnia was defined as the average of the highest 25% of the $EtCO_2$ time course. $\Delta EtCO_2$ was then calculated as their difference. Supplementary Fig. S1 illustrates boundary lines of the top and bottom 25% on the $EtCO_2$ time course of the 4 studies.

To obtain region-of-interest (ROI) CVR values, the T1-MPRAGE image was segmented to obtain a masked image without scalp. This image was further analyzed with BET of FSL to remove residual extracranial tissue (Smith, 2002). The final mask was applied to the CVR data to obtain whole-brain CVR value. For lobar CVR, lobar masks defined on Pickatlas (Lancaster et al., 2000; Maldjian et al., 2003) were applied on the CVR data to obtain values in frontal, temporal, parietal, and occipital lobes as well as subcortical areas.

2.1.3. Statistical analysis

A mixed-effect linear model (Chen et al., 2013) was used to study the dependence of CVR on $bEtCO_2$ and $\Delta EtCO_2$ using data from all 4 studies. The whole-brain CVR was the dependent variable. The $bEtCO_2$ and $\Delta EtCO_2$ were used as fixed-effect independent variables. The study index was used as a random-effect variable. Age was a covariate (Lu et al., 2011). Cohen f^2 effect size was calculated from the mixed-effect linear model using established methods (Selya et al., 2012).

To determine if the dependence of CVR on $bEtCO_2$ and/or $\Delta EtCO_2$ is age-specific, we also examined the interaction terms between age and the $EtCO_2$ measures. Moreover, to examine whether the relationships between CVR and $bEtCO_2$ (or $\Delta EtCO_2$) are different across major brain lobes, we performed additional analyses by including lobes and their interactions with $EtCO_2$ as independent variables.

For all statistical analyses, a p-value of 0.05 or less is considered significant. We performed multiple comparison (Bonferroni) corrections for the lobal data. All analyses were conducted with SPSS v23 (IBM, Armonk, NY).

2.2. Intra-subject variations in CVR and their dependence on end-tidal CO_2

In order to study intra-subject variability, in a subset of subjects (n = 11, those in Study 1 as described in Table 1), the CVR scans were repeated after repositioning. The gap between the two scans was approximately 30 min. This generated two CVR data sets from the same participant.

To examine within-subject $EtCO_2$ effects, within-subject differences in CVR [denoted $\delta(CVR)$], $bEtCO_2$ [$\delta(bEtCO_2)$], and $\Delta EtCO_2$ [$\delta(\Delta EtCO_2)$] were computed between the two sessions. Linear regression analysis was then performed in which $\delta(CVR)$ was the dependent variable and $\delta(bEtCO_2)$ and $\delta(\Delta EtCO_2)$ were the independent variables. The intercept of the linear function was set to be zero as the differences in CVR are expected to be zero when $bEtCO_2$ and $\Delta EtCO_2$ are zeros.

2.3. Numerical simulations

To confirm the experimental findings, numerical simulations were performed to verify the relationship between CVR and $EtCO_2$. The calibrated BOLD model relates CBF and $CMRO_2$ to the BOLD signal using the following equation (Davis et al., 1998; Hoge et al., 1999):

$$BOLD \propto Exp\left(-TE \cdot R_2^*\big|_{dHb}\right)$$
$$= Exp\left(-A \cdot TE \cdot CBV \cdot dHb^\beta\right)$$
$$= Exp\left[-A^{'} \cdot TE \cdot CBF^\alpha \left(\frac{CMRO_2}{CBF}\right)^\beta\right] \quad (3)$$

In Eq. [3], the exponent α describes the coupling relationship between CBF and CBV (Grubb et al., 1974), i.e. $CBV \propto CBF^\alpha$. β is a power-law relationship between venous blood oxygenation and transverse relaxation rate (Ogawa et al., 1992). dHb reflects the oxygen extraction fraction and is related to $CMRO_2/CBF$. In essence, the bracket term indicates that the BOLD signal is modulated by both cerebral blood flow and cerebral metabolic rate (Gauthier and Fan, 2019; Griffeth and Buxton, 2011). If an iso-metabolic assumption is used (but see (Peng et al., 2017; Xu et al., 2011) or non-iso-metabolic reports), the $CMRO_2$ term would reduce to

constant. The BOLD signal is, therefore, a simple function of CBF.

$$BOLD \propto Exp(-K \cdot CBF^{\alpha-\beta}) \qquad (4)$$

where K is $A^{\cdot} \cdot TE \cdot CMRO_2^{\beta}$. In this study, we used four different combinations of α and β values based on widely accepted studies (Bulte et al., 2012; Davis et al., 1998; Griffeth and Buxton, 2011; Merola et al., 2016). For K, we tested a range of values from 2.25 to 4.25 at an interval of 0.5, which yielded BOLD signals in the typical range of CVR experiments.

Furthermore, based on the reported equation (Eq. [5]) between $EtCO_2$ and CBF (Jiang et al., 2019), the BOLD signal can be simulated for each $EtCO_2$ level.

$$CBF = 0.88 \cdot EtCO_2 + 7.65 \qquad (5)$$

CVR, which is defined as BOLD signal change between two $EtCO_2$ levels divided by the $EtCO_2$ change, at any $bEtCO_2$ or $\Delta EtCO_2$ values can then be evaluated.

3. Results

3.1. Relationship between CVR and $EtCO_2$ levels between subjects

Fig. 1c shows the group-averaged CVR map (N = 253). The maps of standard deviation and coefficient-of-variation (COV) are shown in Supplementary Fig. S2. Fig. 2 shows histograms of whole-brain CVR, $bEtCO_2$ and $\Delta EtCO_2$ values in the entire cohort. The fittings of the CO_2 histograms to a Gaussian function are also shown. The CVR has a mean value of 0.190%/mmHg with an intersubject variation (in standard deviation across subjects) of 0.048%/mmHg. The $bEtCO_2$ values had a mean value of 38.1 mmHg and an intersubject variation of 4.3 mmHg. For $\Delta EtCO_2$, the mean and intersubject variations were 9.1 mmHg and 1.9 mmHg, respectively. The basal $EtCO_2$ revealed an age-related decrease (slope = -0.0285 ± 0.0135 mmHg/year, p = 0.036), while $\Delta EtCO_2$ showed an increase with age (slope = 0.0155 ± 0.0058 mmHg/year, p = 0.008). Supplementary Fig. S3 shows scatter plots of CVR, $bEtCO_2$, and $\Delta EtCO_2$, as a function of age.

Linear mixed model analysis that combined data from all studies revealed that whole-brain CVR was significantly correlated with $bEtCO_2$ (slope = -0.0036 ± 0.0008%/mmHg^2, mean $\pm$ SE, p < 0.001) and $\Delta EtCO_2$ (slope = -0.0072 ± 0.0018%/mmHg^2, p < 0.001) (Fig. 3). Their effect size was 0.05 and 0.04, respectively. We also observed an age-related decline in whole-brain CVR (-0.0012 ± 0.0001%/mmHg/year, p < 0.001), similar to those reported in previous literature (Fluck et al., 2014; Lu et al., 2011; McKetton et al., 2018). No interaction effects were observed between age and $bEtCO_2$ (p = 0.20) or between age and
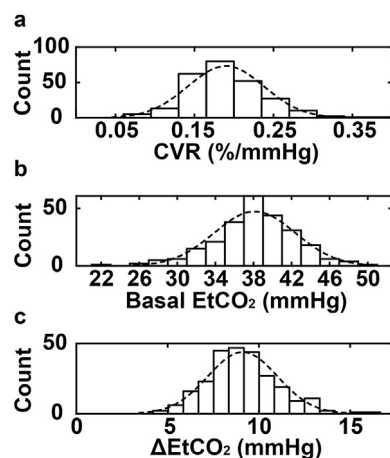
Fig. 2. The distributions of (a) whole-brain CVR, (b) basal $EtCO_2$, and (c) $\Delta EtCO_2$ in the entire cohort (N = 253). The Gaussian fittings of the histograms are also shown.

$\Delta EtCO_2$ (p = 0.96). The random effect size, i.e. CVR differences across studies, was estimated to be 0.026%/mmHg. As a confirmation, we performed linear regression analyses separately for each of the four studies conducted. The results are summarized in Fig. 3. All four studies showed that $bEtCO_2$ and $\Delta EtCO_2$ were inversely associated with whole-brain CVR across subjects, although not all results reached statistical significance.

We also assessed whether the effect of $EtCO_2$ on CVR could be observed in all major brain lobes and whether there were lobe differences in the coefficients. It was found that CVR was significantly associated with $bEtCO_2$ (corrected p < 0.01, combining all studies) and $\Delta EtCO_2$ (corrected p < 0.05, combining all studies) in all lobes examined including frontal, occipital, parietal, temporal, and subcortical gray matter. Fig. 4 plots the coefficients in each lobe when using data from all four studies, with the coefficients from individual studies displayed in Supplementary Fig. S4. The additional comparison indicated that CVR in the occipital lobe had the greatest dependence on $bEtCO_2$ (p < 0.001) and $\Delta EtCO_2$ (p < 0.001) among all major brain lobes.

3.2. Relationship between CVR and $EtCO_2$ levels within a subject

Within-subject variations in CO_2 levels, calculated as standard deviations of the values between two repeated CVR scans, were 0.72 ± 0.59 mmHg (mean $\pm$ SD) and 0.68 ± 0.62 mmHg for $bEtCO_2$ and $\Delta EtCO_2$, respectively. These variation values were lower than those between subjects (3.52 mmHg and 1.78 mmHg for $bEtCO_2$ and $\Delta EtCO_2$, respectively, in the same cohort). There was no significant difference in CVR values between the two repetitions. Linear regression analysis revealed that differences in whole-brain CVR between two repeated scans were inversely associated with both $\delta(bEtCO_2)$ (slope = -0.0171 ± 0.0031%/mmHg^2, p < 0.001) and $\delta(\Delta EtCO_2)$ (slope = -0.0098 ± 0.0031%/mmHg^2, p = 0.012) differences. Their effect size was 3.36 and 1.08, respectively. Fig. 5 shows the partial correlation (after factoring out the other regressor) between differences in CVR and differences in CO_2 levels. We also applied similar analyses to lobar CVR. It was found that within-subject differences in CVR are correlated with $\delta(bEtCO_2)$ and $\delta(\Delta EtCO_2)$ in all major brain lobes. The slopes of these relationships were not different across lobes (p > 0.05), as evaluated by adding the lobe-by-$EtCO_2$ interaction terms to the regression model.

3.3. Numerical simulation results

The assumed relationship between CBF and $EtCO_2$ (Jiang et al., 2019) is shown in Fig. 6a. Based on this formula between CBF and BOLD described in Eq. [3], we simulated the correspondence between BOLD and $EtCO_2$ (Fig. 6b), for a range of coefficient K values.

A non-linear relationship between them can be clearly seen. We then calculated CVR as a function of $bEtCO_2$ for a fixed amount of $\Delta EtCO_2$ (=9 mmHg) and the results are shown in Fig. 6c. An inverse relationship between CVR and $bEtCO_2$ can be seen, in agreement with the experimental results. Similarly, Fig. 6d shows simulation results in which CVR was plotted as a function of $\Delta EtCO_2$ when fixing the $bEtCO_2$ (=38 mmHg). An inverse relationship is observed. To ensure that the simulation results are not dependent on the choice of model parameters, α and β, we repeated the numerical simulations with several other different combinations of α and β (Bulte et al., 2012; Davis et al., 1998; Griffeth and Buxton, 2011; Merola et al., 2016). The results were generally consistent with those shown in Fig. 6. Supplementary Fig. S5 shows simulation results when using several other sets of α and β values.

4. Discussion

The present work examined the influence of basal $EtCO_2$ and hypercapnia-induced $EtCO_2$ change on the measured CVR values in both between-subject and within-subject settings. We found that, in both
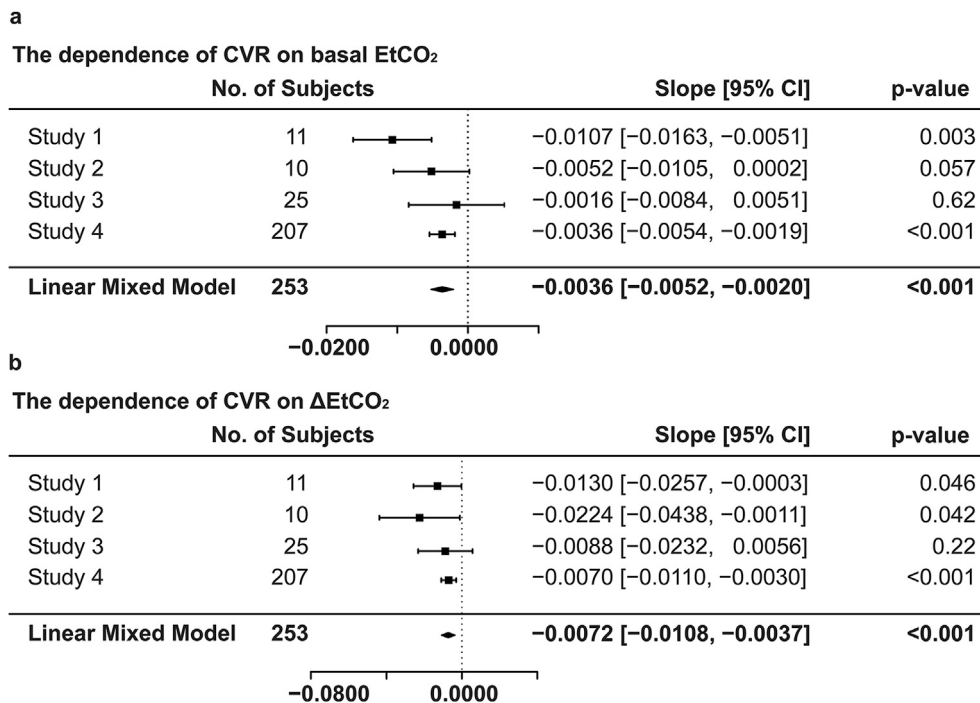
a

The dependence of CVR on basal EtCO$_2$

	No. of Subjects		Slope [95% CI]	p-value
Study 1	11		−0.0107 [−0.0163, −0.0051]	0.003
Study 2	10		−0.0052 [−0.0105, 0.0002]	0.057
Study 3	25		−0.0016 [−0.0084, 0.0051]	0.62
Study 4	207		−0.0036 [−0.0054, −0.0019]	<0.001
Linear Mixed Model	**253**		**−0.0036 [−0.0052, −0.0020]**	**<0.001**

−0.0200   0.0000

b

The dependence of CVR on ΔEtCO$_2$

	No. of Subjects		Slope [95% CI]	p-value
Study 1	11		−0.0130 [−0.0257, −0.0003]	0.046
Study 2	10		−0.0224 [−0.0438, −0.0011]	0.042
Study 3	25		−0.0088 [−0.0232, 0.0056]	0.22
Study 4	207		−0.0070 [−0.0110, −0.0030]	<0.001
Linear Mixed Model	**253**		**−0.0072 [−0.0108, −0.0037]**	**<0.001**

−0.0800   0.0000

Fig. 3. Summary of the dependence of CVR on (a) basal EtCO$_2$ and (b) ΔEtCO$_2$ when considering each study separately and when combining all data.
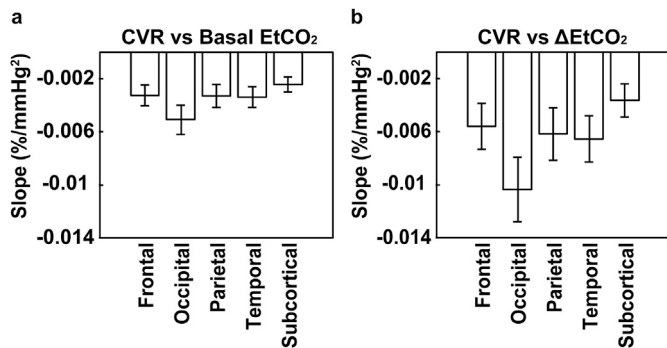

Fig. 4. The slope of the CVR dependence on CO$_2$ in major brain lobes. (a) Slope between CVR and basal EtCO$_2$. (b) Slope between CVR and ΔEtCO$_2$.
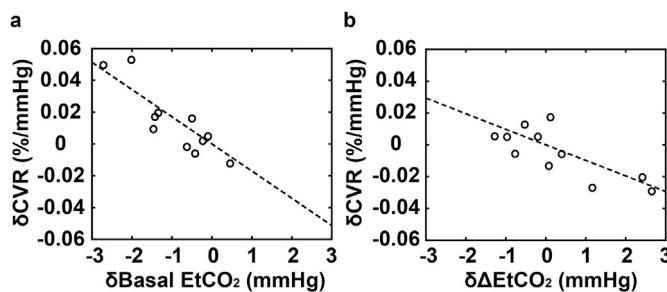

Fig. 5. Scatter plot between CVR and EtCO$_2$ variations in a within-subject setting. The x-axis shows the differences in EtCO$_2$ between two sessions. The y-axis shows the differences in CVR between two sessions. (a) shows the basal EtCO$_2$ effect. (b) shows the ΔEtCO$_2$ effect. Because the CVR difference is dependent on both basal EtCO$_2$ and ΔEtCO$_2$ differences, we factored out the other regressor and re-referenced to its zero value before plotting the scatter plot.

Fig. 6. Numerical simulation results. (a) Assumed relationship between EtCO$_2$ and CBF that is used in the simulation. (b) Absolute BOLD signal as a function of EtCO$_2$. The BOLD signal here indicates the MR signal intensity obtained from the EPI-based T2*-weighted pulse sequence. (c) CVR as a function of basal EtCO$_2$. (d) CVR as a function of ΔEtCO$_2$. α = 0.14, β = 0.91 (Griffeth and Buxton, 2011).

settings, higher basal EtCO$_2$ and greater EtCO$_2$ change in CVR experiments are associated with lower CVR values. The present work suggests that both basal physiological state and the level of hypercapnic stimulus
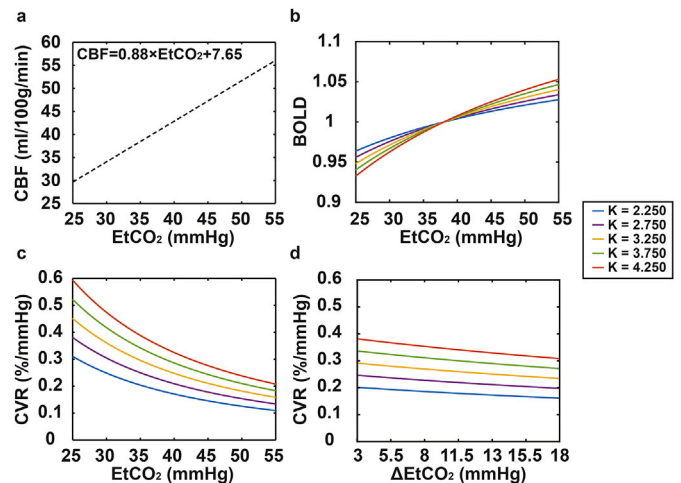
intensity should be considered in application studies of CVR, to reduce inter-subject and intra-subject variations in the data.

The observed dependence of CVR on EtCO$_2$ can be attributed to the BOLD signal mechanism. The BOLD signal difference is associated with changes in venous oxygenation between the basal state and the hypercapnic state. The larger the venous oxygenation change, the greater the BOLD signal difference (i.e. CVR). However, the venous oxygenation level can only go as high as 100%, thus this value will reach a plateau at high EtCO$_2$. That is, in the high EtCO$_2$ range, each unit of EtCO$_2$ increase will result in a small BOLD signal change. This "plateau" phenomenon is well-known in the fMRI field from both between-subject (Lu et al., 2008) and within-subject (Cohen et al., 2002; Xu et al., 2011) point-of-view. The present study extends this relationship of BOLD-versus-basal

physiology to CVR results. Our numerical simulations provided an additional, more quantitative illustration of this notion. Although the figure shown (Fig. 6) was based on one set of α and β values, we have conducted additional simulations using other values and all results showed an inverse dependence of CVR on bEtCO$_2$ and ΔEtCO$_2$ (Supplementary Fig. S5). Another possible mechanism for the dependence of CVR on EtCO$_2$ could be related to the non-linear relationship between EtCO$_2$ and CBF itself. As basal CO$_2$ level is raised and a blood vessel dilates accordingly, the vascular reserve is diminished. Thus, the further hypercapnic challenge will elicit smaller vasodilation. This may be another explanation underlying the inverse relationship between CVR and CO$_2$. We also want to point out that the CVR measure reported in this study was calculated as BOLD signal change per mmHg change in EtCO$_2$. Thus, the actual CO$_2$ change induced by hypercapnic breathing has been considered in the CVR quantification.

As CVR MRI receives increasing attention in recent years, the impact of experimental condition on the CVR measurement has been becoming a topic of great interest. Using a ramp CO$_2$ paradigm, Bhogal et al. (2014) showed that the relationship between BOLD signal and EtCO$_2$ was, in fact, non-linear and that the actual CVR values measured were dependent on the range of EtCO$_2$ values studied in the experiment. van Niftrik et al. (2018) showed that, when comparing two groups of healthy subjects in whom one group was measured at their natural level of CO$_2$ while the other group was studied under raised CO$_2$ level, the elevated-CO$_2$ group revealed a lower CVR value compared to the natural-level group. While these findings are not directly comparable to our study, the general observation that a higher basal CO$_2$ corresponds to a lower CVR is consistent with the data in the present study. Bright et al. (2011), Halani et al. (2015) and De Vis et al. (2018) have studied the effect of basal state on CVR measurement in an intra-subject setting, again by elevating the subject's basal CO$_2$ level. The results were not coherent, with some studies showing an absence of effect of basal CO$_2$ on CVR while others suggesting a trend of reduction in selected brain regions. We note that all of the subjects in the present study were studied under their natural basal states. Owing to the large sample size afforded in this analysis, we were able to show a definitive ($p < 0.001$) inverse correlation between CVR and basal EtCO$_2$. This relationship was observed throughout the brain. Furthermore, we showed that there was an inverse correlation between CVR and ΔEtCO$_2$, a parameter that has received less attention in the previous literatures.

The findings from the present study have several implications for basic science and clinical applications of CVR MRI. First, it should be recognized that much of the "noise" in CVR data is physiological, rather than thermal noise, such as the CO$_2$-level related variations described in the present study. These noise sources, once understood, can be corrected or reduced. For example, for the EtCO$_2$ and ΔEtCO$_2$ related variations, one can use the slopes reported in this study (i.e. 0.0036%/mmHg^2 for bEtCO$_2$ and 0.0072%/mmHg^2 for ΔEtCO$_2$) to correct the CVR values before subjecting them to statistical analysis of patients-versus-controls or before-versus-after treatment. An alternative approach to account for the CO$_2$ effect is to include bEtCO$_2$ and ΔEtCO$_2$ in the regression model as covariates. Both methods can be used if one does not expect a systematic difference in CO$_2$ levels between the patient and control groups. On the other hand, for clinical studies in which CO$_2$ levels may be altered by disease, e.g. sleep apnea or chronic obstructive pulmonary disease (COPD), the slope-correction method is recommended to avoid variable co-linearity in the regression model. Given the observed influence of EtCO$_2$ and ΔEtCO$_2$ on CVR, another approach to minimize these effects is to use CO$_2$ clamping technique so that every participant has the same basal CO$_2$ and CO$_2$ change (Fisher, 2016; Slessarev et al., 2007). However, one issue is that each individual presumably has their own "operating" CO$_2$ level in their daily life. In fact, the present study and others have shown that the "operating" CO$_2$ level varies with age, and other factors (Cantin et al., 2011; Dhokalia et al., 1998). Thus, experimental alternation of their basal CO$_2$ level may cause profound changes in their brain and respiratory physiology. These changes and the

associated compensatory responses may result in a CVR value that is dramatically different from their natural breathing state. This is relevant to the choice of CVR experimental apparatus that has stimulated some discussions in the field. One type of stimulus apparatus, generally referred to as fixed inspired CO$_2$ system (Bulte et al., 2009; Driver et al., 2016; Lajoie et al., 2016; Lu et al., 2014), delivers a fixed concentration of CO$_2$ to the subject and, because different subjects have different ventilation rate/volume as well as in their responses to CO$_2$ gas, the actual EtCO$_2$ and its change during CVR experiments are different across subjects. Another type of system uses a feedback loop to control the EtCO$_2$ of the subject so that every subject has the same basal EtCO$_2$ (e.g. 40 mmHg) and EtCO$_2$ change (e.g. 10 mmHg) during the experiment (Fisher, 2016; Slessarev et al., 2007). The benefits and limitations of each system have been under some debate. The present work shows that clamping or modulating the subject's EtCO$_2$ to a level different from their natural state will result in a difference in the measured value. However, it remains to be determined whether these modulated CVR values would reveal less or more variations within a supposedly homogeneous group of participants. This question should be investigated in future studies. Finally, one can consider using CBF-based techniques such as arterial-spin-labeling (ASL) for CVR measurement. However, ASL-CVR has its own challenges such as low signal-to-noise ratio (SNR) (Halani et al., 2015; Ho et al., 2011), sensitivity to bolus-arrival-time change during hypercapnia (Ho et al., 2011; Su et al., 2017), and potential changes in labeling efficiency when arterial flow velocity is increased (Aslan et al., 2010).

Our lobar analysis revealed that there were some differences in the slope of the relationship between CVR and EtCO$_2$ and that the occipital lobe had the greatest slope values. Interestingly, previous studies have shown that the occipital lobe also had the highest CVR values among all major brain lobes (Yezhuvath et al., 2009; Zhou et al., 2015). Given that the occipital lobe was adjacent to large venous sinuses, we also performed additional analysis to erode the ROI mask to remove the sinus voxels, and found that the CVR-vs-CO$_2$ slope was minimally affected by the erosion.

In this study, the basal and hypercapnic CO$_2$ levels were defined as the bottom and top 25% of the EtCO$_2$ time course. We have also tried several other approaches to define these values, including using 15% and 5% of the time course, using the peak values, and using the average of the first 20 time points as baseline while using the average of the values during the time window corresponding to the CO$_2$ breathing block as hypercapnic EtCO$_2$. The findings on the relationship between CVR and basal EtCO$_2$/ΔEtCO$_2$ were the same. Supplementary Table S1 shows coefficients and p-values of these additional analyses.

In the within-subject variation study, there was a difference in basal EtCO$_2$ between the two scans. Basal EtCO$_2$ during session two appeared to be lower than that during session one ($p = 0.008$). We therefore further investigated the nature of this decrease. Supplemental Fig. S6 shows the group-averaged EtCO$_2$ time courses of the two sessions. It can be seen that the basal EtCO$_2$ of the two sessions started at approximately the same levels, but session 2 seems to show a gradual decrease over blocks. This may be due to fatigue of the participants in the latter session. Further investigation is needed to confirm and understand this effect.

Several limitations of the current study should be acknowledged. First, the four studies conducted in this work used slightly different imaging parameters such as TE, voxel size, CO$_2$ block number, and scan time. Since BOLD percentage signal change, thereby CVR, is known to be affected by TE (Lu and van Zijl, 2005), there may be systematic heterogeneities in the data. However, we should note that our linear regression was based on a mixed-effect model where the study index was used as a random-effect variable, thus data from each study were treated as independent groups. Second, although the group results were significant, there were discrepancies in their results for individual studies. Furthermore, the effect sizes of EtCO$_2$ and ΔEtCO$_2$ (0.05 and 0.04, respectively) in the between-subject data are still relatively small, thus their practical utility is unclear. The within-subject effect sizes (3.36 and 1.08) are

greater, thus may be useful in comparison of CVR before and after intervention or follow-up. Third, while we have high confidence in the presence of an inverse relationship between CVR and $EtCO_2$ ($p < 0.001$), the slope value (i.e. $bEtCO_2$ slope $= -0.0036 \pm 0.0008$ %/mmHg^2, $\Delta EtCO_2$ slope $= -0.0072 \pm 0.0018$ %/mmHg^2) still contains certain degree of uncertainties (about 25% of the estimated values). Thus, more data are needed to determine the exact values of the slope variables as well as their dependence on population, e.g. through a meta-analysis. Similarly, it should be kept in mind that these slope values are for 3 T and may not be valid for other field strengths such as 1.5T or 7T. Finally, the present study has only examined CVR data from healthy controls. The extent to which the relationship between CVR and $EtCO_2$ can be observed in diseased populations requires further investigation. Relevant to this point, Study 3 only showed a trend of $EtCO_2$ effects on CVR and one possible reason is that participants in Study 3 were all elderly subjects and many of them have commonly vascular risks such as hypertension, hypercholesterolemia, etc.

5. Conclusions

CVR, as typically quantified by BOLD MRI signal change per unit change in $EtCO_2$, was found to be dependent on the physiological state of the individual. Specifically, CVR was lower in individuals with a higher basal $EtCO_2$ and/or with a greater $EtCO_2$ change upon hypercapnia. Similarly, within the same individual, the measured CVR value was lower if their basal $EtCO_2$ or $\Delta EtCO_2$ during that particular scan session were greater. These observations have important implications in understanding physiological noise in CVR data and in applying CVR MRI to clinical studies. Potential approaches to use these findings to reduce noise and augment sensitivity have been proposed.

Acknowledgments

Appendix A. Supplementary data

Supplementary data to this article can be found online at https://doi.org/10.1016/j.neuroimage.2019.116365.

References

Aslan, S., Xu, F., Wang, P.L., Uh, J., Yezhuvath, U.S., van Osch, M., Lu, H., 2010. Estimation of labeling efficiency in pseudocontinuous arterial spin labeling. Magn. Reson. Med. 63, 765–771.

Bhogal, A.A., Siero, J.C., Fisher, J.A., Froeling, M., Luijten, P., Philippens, M., Hoogduin, H., 2014. Investigating the non-linearity of the BOLD cerebrovascular reactivity response to targeted hypo/hypercapnia at 7T. Neuroimage 98, 296–305.

Bright, M.G., Croal, P.L., Blockley, N.P., Bulte, D.P., 2017. Multiparametric measurement of cerebral physiology using calibrated fMRI. Neuroimage.

Bright, M.G., Donahue, M.J., Duyn, J.H., Jezzard, P., Bulte, D.P., 2011. The effect of basal vasodilation on hypercapnic and hypocapnic reactivity measured using magnetic resonance imaging. J. Cereb. Blood Flow Metab. 31, 426–438.

Bright, M.G., Murphy, K., 2013. Reliable quantification of BOLD fMRI cerebrovascular reactivity despite poor breath-hold performance. Neuroimage 83, 559–568.

Bulte, D.P., Drescher, K., Jezzard, P., 2009. Comparison of hypercapnia-based calibration techniques for measurement of cerebral oxygen metabolism with MRI. Magn. Reson. Med. 61, 391–398.

Bulte, D.P., Kelly, M., Germuska, M., Xie, J., Chappell, M.A., Okell, T.W., Bright, M.G., Jezzard, P., 2012. Quantitative measurement of cerebral physiology using respiratory-calibrated MRI. Neuroimage 60, 582–591.

Cantin, S., Villien, M., Moreaud, O., Tropres, I., Keignart, S., Chipon, E., Le Bas, J.F., Warnking, J., Krainik, A., 2011. Impaired cerebral vasoreactivity to CO2 in Alzheimer's disease using BOLD fMRI. Neuroimage 58, 579–587.

Chan, S.T., Evans, K.C., Rosen, B.R., Song, T.Y., Kwong, K.K., 2015. A case study of magnetic resonance imaging of cerebrovascular reactivity: a powerful imaging marker for mild traumatic brain injury. Brain Inj. 29, 403–407.

Chen, G., Saad, Z.S., Britton, J.C., Pine, D.S., Cox, R.W., 2013. Linear mixed-effects modeling approach to FMRI group analysis. Neuroimage 73, 176–190.

Chen, J.J., 2018. Functional MRI of brain physiology in aging and neurodegenerative diseases. Neuroimage.

Cohen, E.R., Ugurbil, K., Kim, S.G., 2002. Effect of basal conditions on the magnitude and dynamics of the blood oxygenation level-dependent fMRI response. J. Cereb. Blood Flow Metab. 22, 1042–1053.

Davis, T.L., Kwong, K.K., Weisskoff, R.M., Rosen, B.R., 1998. Calibrated functional MRI: mapping the dynamics of oxidative metabolism. Proc. Natl. Acad. Sci. U. S. A. 95, 1834–1839.

De Vis, J.B., Bhogal, A.A., Hendrikse, J., Petersen, E.T., Siero, J.C.W., 2018. Effect sizes of BOLD CVR, resting-state signal fluctuations and time delay measures for the assessment of hemodynamic impairment in carotid occlusion patients. Neuroimage 179, 530–539.

De Vis, J.B., Petersen, E.T., Bhogal, A., Hartkamp, N.S., Klijn, C.J., Kappelle, L.J., Hendrikse, J., 2015. Calibrated MRI to evaluate cerebral hemodynamics in patients with an internal carotid artery occlusion. J. Cereb. Blood Flow Metab. 35, 1015–1023.

Dhokalia, A., Parsons, D.J., Anderson, D.E., 1998. Resting end-tidal CO2 association with age, gender, and personality. Psychosom. Med. 60, 33–37.

Driver, I.D., Whittaker, J.R., Bright, M.G., Muthukumaraswamy, S.D., Murphy, K., 2016. Arterial CO2 fluctuations modulate neuronal rhythmicity: implications for MEG and fMRI studies of resting-state networks. J. Neurosci. 36, 8541–8550.

Fierstra, J., Sobczyk, O., Battisti-Charbonney, A., Mandell, D.M., Poublanc, J., Crawley, A.P., Mikulis, D.J., Duffin, J., Fisher, J.A., 2013. Measuring cerebrovascular reactivity: what stimulus to use? J. Physiol. 591, 5809–5821.

Fierstra, J., van Niftrik, B., Piccirelli, M., Burkhardt, J.K., Pangalu, A., Kocian, R., Valavanis, A., Weller, M., Regli, L., Bozinov, O., 2016. Altered intraoperative cerebrovascular reactivity in brain areas of high-grade glioma recurrence. Magn. Reson. Imaging 34, 803–808.

Fisher, J.A., 2016. The CO2 stimulus for cerebrovascular reactivity: fixing inspired concentrations vs. targeting end-tidal partial pressures. J. Cereb. Blood Flow Metab. 36, 1004–1011.

Fluck, D., Beaudin, A.E., Steinback, C.D., Kumarpillai, G., Shobha, N., McCreary, C.R., Peca, S., Smith, E.E., Poulin, M.J., 2014. Effects of aging on the association between cerebrovascular responses to visual stimulation, hypercapnia and arterial stiffness. Front. Physiol. 5, 49.

Gauthier, C.J., Fan, A.P., 2019. BOLD signal physiology: models and applications. Neuroimage 187, 116–127.

Gauthier, C.J., Hoge, R.D., 2013. A generalized procedure for calibrated MRI incorporating hyperoxia and hypercapnia. Hum. Brain Mapp. 34, 1053–1069.

Geranmayeh, F., Wise, R.J., Leech, R., Murphy, K., 2015. Measuring vascular reactivity with breath-holds after stroke: a method to aid interpretation of group-level BOLD signal changes in longitudinal fMRI studies. Hum. Brain Mapp. 36, 1755–1771.

Griffeth, V.E., Buxton, R.B., 2011. A theoretical framework for estimating cerebral oxygen metabolism changes using the calibrated-BOLD method: modeling the effects of blood volume distribution, hematocrit, oxygen extraction fraction, and tissue signal properties on the BOLD signal. Neuroimage 58, 198–212.

Grubb Jr., R.L., Raichle, M.E., Eichling, J.O., Ter-Pogossian, M.M., 1974. The effects of changes in PaCO2 on cerebral blood volume, blood flow, and vascular mean transit time. Stroke 5, 630–639.

Halani, S., Kwinta, J.B., Golestani, A.M., Khatamian, Y.B., Chen, J.J., 2015. Comparing cerebrovascular reactivity measured using BOLD and cerebral blood flow MRI: the effect of basal vascular tension on vasodilatory and vasoconstrictive reactivity. Neuroimage 110, 110–123.

Ho, Y.C., Petersen, E.T., Zimine, I., Golay, X., 2011. Similarities and differences in arterial responses to hypercapnia and visual stimulation. J. Cereb. Blood Flow Metab. 31, 560–571.

Hoge, R.D., Atkinson, J., Gill, B., Crelier, G.R., Marrett, S., Pike, G.B., 1999. Investigation of BOLD signal dependence on cerebral blood flow and oxygen consumption: the deoxyhemoglobin dilution model. Magn. Reson. Med. 42, 849–863.

Hou, X., Liu, P., Gu, H., Chan, M., Li, Y., Peng, S.L., Wig, G., Yang, Y., Park, D., Lu, H., 2019. Estimation of brain functional connectivity from hypercapnia BOLD MRI data: validation in a lifespan cohort of 170 subjects. Neuroimage 186, 455–463.

Jiang, D., Li, Y., Lin, Z., Sur, S., Liu, P., Xu, C., Hazel, K., Pottanat, G., Yasar, S., Rosenberg, P., Albert, M., Lu, H., 2019. Physiological underpinnings of variations in CBF measured by pCASL MRI. Workshop Arter. Spin Labeling MRI: Tech. Updates Clin. Exp. 26.

Lajoie, I., Tancredi, F.B., Hoge, R.D., 2016. Regional reproducibility of BOLD calibration parameter M, OEF and resting-state CMRO2 measurements with QUO2 MRI. PLoS One 11.

Lancaster, J.L., Woldorff, M.G., Parsons, L.M., Liotti, M., Freitas, C.S., Rainey, L., Kochunov, P.V., Nickerson, D., Mikiten, S.A., Fox, P.T., 2000. Automated Talairach atlas labels for functional brain mapping. Hum. Brain Mapp. 10, 120–131.

Liu, P., Welch, B.G., Li, Y., Gu, H., King, D., Yang, Y., Pinho, M., Lu, H., 2017. Multiparametric imaging of brain hemodynamics and function using gas-inhalation MRI. Neuroimage 146, 715–723.

Liu, P.Y., De Vis, J.B., Lu, H.Z., 2019. Cerebrovascular reactivity (CVR) MRI with CO2 challenge: a technical review. Neuroimage 187, 104–115.

Liu, P.Y., Hebrank, A.C., Rodrigue, K.M., Kennedy, K.M., Section, J., Park, D.C., Lu, H.Z., 2013. Age-related differences in memory-encoding fMRI responses after accounting for decline in vascular reactivity. Neuroimage 78, 415–425.

Lu, H., Liu, P., Yezhuvath, U., Cheng, Y., Marshall, O., Ge, Y., 2014. MRI mapping of cerebrovascular reactivity via gas inhalation challenges. J. Vis. Exp.

Lu, H., van Zijl, P.C., 2005. Experimental measurement of extravascular parenchymal BOLD effects and tissue oxygen extraction fractions using multi-echo VASO fMRI at 1.5 and 3.0 T. Magn. Reson. Med. 53, 808–816.

Lu, H., Xu, F., Rodrigue, K.M., Kennedy, K.M., Cheng, Y., Flicker, B., Hebrank, A.C., Uh, J., Park, D.C., 2011. Alterations in cerebral metabolic rate and blood supply across the adult lifespan. Cerebr. Cortex 21, 1426–1434.

Lu, H.Z., Zhao, C.G., Ge, Y.L., Lewis-Amezcua, K., 2008. Baseline blood oxygenation modulates response amplitude: physiologic basis for intersubject variations in functional MRI signals. Magn. Reson. Med. 60, 364–372.

Maldjian, J.A., Laurienti, P.J., Kraft, R.A., Burdette, J.H., 2003. An automated method for neuroanatomic and cytoarchitectonic atlas-based interrogation of fMRI data sets. Neuroimage 19, 1233–1239.

Mandell, D.M., Han, J.S., Poublanc, J., Crawley, A.P., Stainsby, J.A., Fisher, J.A., Mikulis, D.J., 2008. Mapping cerebrovascular reactivity using blood oxygen level-dependent MRI in Patients with arterial steno-occlusive disease: comparison with arterial spin labeling MRI. Stroke 39, 2021–2028.

Marshall, O., Lu, H.Z., Brisset, J.C., Xu, F., Liu, P.Y., Herbert, J., Grossman, R.I., Ge, Y.L., 2014. Impaired cerebrovascular reactivity in multiple sclerosis. Jama Neurol. 71, 1275–1281.

McKetton, L., Sobczyk, O., Duffin, J., Poublanc, J., Sam, K., Crawley, A.P., Venkatraghavan, L., Fisher, J.A., Mikulis, D.J., 2018. The aging brain and cerebrovascular reactivity. Neuroimage 181, 132–141.

Merola, A., Murphy, K., Stone, A.J., Germuska, M.A., Griffeth, V.E.M., Blockley, N.P., Buxton, R.B., Wise, R.G., 2016. Measurement of oxygen extraction fraction (OEF): an optimized BOLD signal model for use with hypercapnic and hyperoxic calibration. Neuroimage 129, 159–174.

Murphy, K., Harris, A.D., Wise, R.G., 2011. Robustly measuring vascular reactivity differences with breath-hold: normalising stimulus-evoked and resting state BOLD fMRI data. Neuroimage 54, 369–379.

Ogawa, S., Tank, D.W., Menon, R., Ellermann, J.M., Kim, S.G., Merkle, H., Ugurbil, K., 1992. Intrinsic signal changes accompanying sensory stimulation: functional brain mapping with magnetic resonance imaging. Proc. Natl. Acad. Sci. U. S. A. 89, 5951–5955.

Peng, S.L., Chen, X., Li, Y., Rodrigue, K.M., Park, D.C., Lu, H., 2018. Age-related changes in cerebrovascular reactivity and their relationship to cognition: a four-year longitudinal study. Neuroimage 174, 257–262.

Peng, S.L., Ravi, H., Sheng, M., Thomas, B.P., Lu, H.Z., 2017. Searching for a truly "iso-metabolic' gas challenge in physiological MRI. J. Cereb. Blood Flow Metab. 37, 715–725.

Ravi, H., Thomas, B.P., Peng, S.L., Liu, H.L., Lu, H.Z., 2016. On the optimization of imaging protocol for the mapping of cerebrovascular reactivity. J. Magn. Reson. Imaging 43, 661–668.

Selya, A.S., Rose, J.S., Dierker, L.C., Hedeker, D., Mermelstein, R.J., 2012. A practical guide to calculating Cohen's f(2), a measure of local effect size, from PROC MIXED. Front. Psychol. 3.

Slessarev, M., Han, J., Mardimae, A., Prisman, E., Preiss, D., Volgyesi, G., Ansel, C., Duffin, J., Fisher, J.A., 2007. Prospective targeting and control of end-tidal CO2 and O2 concentrations. J. Physiol. 581, 1207–1219.

Smith, S.M., 2002. Fast robust automated brain extraction. Hum. Brain Mapp. 17, 143–155.

Sobczyk, O., Battisti-Charbonney, A., Fierstra, J., Mandell, D.M., Poublanc, J., Crawley, A.P., Mikulis, D.J., Duffin, J., Fisher, J.A., 2014. A conceptual model for CO(2)-induced redistribution of cerebral blood flow with experimental confirmation using BOLD MRI. Neuroimage 92, 56–68.

Su, P., Mao, D., Liu, P., Li, Y., Pinho, M.C., Welch, B.G., Lu, H., 2017. Multiparametric estimation of brain hemodynamics with MR fingerprinting ASL. Magn. Reson. Med. 78, 1812–1823.

Tancredi, F.B., Hoge, R.D., 2013. Comparison of cerebral vascular reactivity measures obtained using breath-holding and CO2 inhalation. J. Cereb. Blood Flow Metab. 33, 1066–1074.

Taneja, K., Lu, H.Z., Welch, B.G., Thomas, B.P., Pinho, M., Lin, D., Hillis, A.E., Liu, P.Y., 2019. Evaluation of cerebrovascular reserve in patients with cerebrovascular diseases using resting-state MRI: a feasibility study. Magn. Reson. Imag. 59, 46–52.

Thomas, B.P., Liu, P.Y., Asian, S., King, K.S., van Osch, M.J.P., Lu, H.Z., 2013. Physiologic underpinnings of negative BOLD cerebrovascular reactivity in brain ventricles. Neuroimage 83, 505–512.

van Niftrik, C.H.B., Piccirelli, M., Bozinov, O., Maldaner, N., Strittmatter, C., Pangalu, A., Valavanis, A., Regli, L., Fierstra, J., 2018. Impact of baseline CO2 on Blood-Oxygenation-Level-Dependent MRI measurements of cerebrovascular reactivity and task-evoked signal activation. Magn. Reson. Imaging 49, 123–130.

Xu, F., Uh, J., Brier, M.R., Hart Jr., J., Yezhuvath, U.S., Gu, H., Yang, Y., Lu, H., 2011. The influence of carbon dioxide on brain activity and metabolism in conscious humans. J. Cereb. Blood Flow Metab. 31, 58–67.

Yezhuvath, U.S., Lewis-Amezcua, K., Varghese, R., Xiao, G., Lu, H., 2009. On the assessment of cerebrovascular reactivity using hypercapnia BOLD MRI. NMR Biomed. 22, 779–786.

Yezhuvath, U.S., Uh, J., Cheng, Y.M., Martin-Cook, K., Weiner, M., Diaz-Arrastia, R., van Osch, M., Lu, H.Z., 2012. Forebrain-dominant deficit in cerebrovascular reactivity in Alzheimer's disease. Neurobiol. Aging 33, 75–82.

Zhou, Y., Rodgers, Z.B., Kuo, A.H., 2015. Cerebrovascular reactivity measured with arterial spin labeling and blood oxygen level dependent techniques. Magn. Reson. Imaging 33, 566–576.